D E P A R T M E N T O F M A T H E M A T I C S

AN ADAPTIVE TIME STEPPING STRATEGY FOR THE **ASWR** SEMICONDUCTOR DIFFUSION MODEL SIMULATOR

K. Chen, M. J. Baines and P. K. Sweby

Numerical Analysis Report **11/91**

Whiteknights, P. O. Box 220,

Reading RG6 2AX, Berkshire.

U N I V E R S I T Y O F R E A D I N G

Abstract

A new time step selection procedure is proposed for the ASWR finite element code of Lorenz and Svoboda [7] for 2D semiconductor process modelling diffusion equations. The strategy is based on equidistributing the local truncation errors of the numerical scheme. The use of B-splines for interpolation (as well as for trial space) results in a banded and diagonally dominant matrix. The approximate inverse of such a matrix can be accurately provided by another band matrix, which in turn can be used to work out the *approximate* finite difference scheme corresponding to the ASWR finite element method and further to calculate estimates of the local truncation errors of the numerical scheme. Numerical experiments on six full simulation problems have been carried out. Results show that our proposed strategy is more efficient, and better conserves the total mass.

Key words : Semiconductor process modelling, Nonlinear parabolic PDE's, Blended B-splines, Finite difference methods (FDM's), Petrov-Galerkin methods (FEM's), Predictor corrector schemes, Automatic time step selection.

AMS (MOS) Subject Classifications : 65M60, 35K57, 35K15.

Contents

1 Introduction

In [1] we presented numerical methods for the solution of 1D nonlinear semiconductor diffusion equations, and in particular introduced a practical time stepping strategy for the scheme used. There both finite difference methods and finite element methods were used for the spatial discretization.

Here we continue our study by extending previous 1D results to 2D nonlinear equations for semiconductor process modelling simulation. Implementation of our new time stepping strategy into the ASWR finite element code of [7] has been completed; we report on the test results of performance of the modified ASWR code on some full 2D simulation problems. The code is capable of simulating, among other processes, 2D dopant diffusion of Antimony, Arsenic, Boron and Phosphorus for either one dopant or multiple dopants.

We first state the equations which will be considered here. For an r-dopant diffusion problem in a silicon medium Ω, the concentrations of dopants in Ω at time t may be described by

$$\frac{\partial C_k}{\partial t} = \mathrm{Div}\left[D_k \mathrm{grad} C_k + Z_k C_k \mathrm{grad}\Phi\right] \qquad k = 1, \cdots, r \tag{1}$$

where $C_k = C_k(x, y, t)$ is the concentration for the k-th dopant, D_k is the diffusion coefficient, $Z_k = \pm 1$ depends on the dopant used (-1 for singly ionized acceptors, $+1$ for donors) and $\Phi = \Phi(\sum Z_k C_k)$ is the electrostatic potential. Denote by $C = \sum_{k=1}^{r} Z_k C_k$ the total concentration. Then the potential function is calculated by $\Phi = \log(n/n_i)$ where

$$n = \frac{1}{2}\left(C + \sqrt{C^2 + 4n_i^2}\right)$$

is the electron concentration and n_i is the intrinsic electron concentration at the process

temperature. As in [1], the transformation of $f_k = \log C_k$ will convert (1) to the following system

$$\frac{\partial f_k}{\partial t} = \mathcal{L}_k f_k, \qquad k = 1, \cdots, r \tag{2}$$

where $\mathcal{L}_k f_k = \mathrm{Div}\,[D_k \mathrm{grad}(f_k + Z_k\Phi)] + \mathrm{grad} f_k \cdot \mathrm{grad}(f_k + Z_k\Phi)$ depends on $f_1, \cdots, f_r$. It is this system which we shall solve in what follows.

The time step selection is an important step in ensuring efficiency of numerical methods. There are not many strategies that are readily available. In the literature on solving nonlinear partial differential equations of parabolic type, the traditional method of lines is usually used and further time step selection is determined by methods adopted for solving the system of ordinary differential equations. See Eriksson et al [3] and Lambert [5]. This means that we have to solve a nonlinear system of algebraic equations for a typical implicit time stepping (refer to §3). Even so, it is generally difficult to find a robust strategy for time steps.

Consequently for many practical codes, it is common to use fixed time step sizes or heuristic time step selection procedures. For example, see Kreskovsky et al [4] and O'Brien et al [9].

Here for a particular time stepping scheme, we propose a strategy for automatic time step selection. The idea applies in principle to other schemes as well. It is based on equidistributing local truncation errors (LTE's) in time and space discretizations. Therefore it is readily applicable to finite difference methods since such error estimates can be found. For finite element methods using B-spline basis, we shall show that good approximations to LTE's are always possible so that our proposed strategy can be applied.

In §2 we discuss the finite element discretization of (2). In §3 we introduce a three-level predictor-corrector scheme for the temporal discretization and linearization of (2) and further investigate its (linear) stability property. In §4 we use the idea of approximate inversion to find an explicit and approximate finite difference form of the underlying finite element method, and then carry out the local truncation error (LTE) analysis. Using the LTE estimates, we describe in §5 two adaptive time stepping strategies either of which can automatically select the time step. Here the second approach is designed specifically for conservation of the total mass, which is of physical importance. Numerical experiments on six full simulation problems are presented in §6.

2 Finite element solution

For simplicity, let us assume that the domain of interest is the unit rectangular region $\Omega = [0,1] \times [0,1]$. More general boundaries may be considered similarly. Divide the domain Ω into $N \times N$ boxes $\Omega_{lm} = [x_{l-1}, x_l] \times [y_{m-1}, y_m]$ $(l, m = 1, \cdots, N)$. Then we choose a Petrov-Galerkin finite method which uses as

test space :

$$S_1 = \text{span}\{\phi_{lm} \mid l, m = 1, \cdots, N\}$$

and trial space :

$$S_2 = \text{span}\{D_{ik} \mid i, k = 0, \cdots, N+1\}$$

where

$$\phi_{lm} = \begin{cases} 1 & (x,y) \in \Omega_{lm} \\ 0 & \text{otherwise} \end{cases}$$

and the D_{ik}'s are chosen from blending the 1D quadratic B-splines (as defined in [1])

$$D_{ik}(x,y) = \bar{B}_{km} B_i(x) + \bar{B}_{il} B_k(y) - \bar{B}_{km} \bar{B}_{il}$$

where

$$\bar{B}_{km} = \frac{1}{(h_y)_m} \int_{y_{m-1}}^{y_m} B_k(y) dy \qquad \text{and} \qquad \bar{B}_{il} = \frac{1}{(h_x)_l} \int_{x_{l-1}}^{x_l} B_i(x) dx$$

The resulting finite element method (called ASWR in [7]) finds the solution

$$F_k = \sum_{i=0}^{N+1} \sum_{j=0}^{N+1} \alpha_{k,ij} D_{ij}(x,y), \qquad \text{for } k = 1, \cdots, r \tag{3}$$

from S_2 by solving

$$\left\langle \frac{\partial F_k}{\partial t} - \mathcal{L}_k F_k,\ \omega \right\rangle = 0, \qquad \forall \omega \in S_1$$

i.e.

$$\int_{\Omega_{lm}} \left(\frac{\partial F_k}{\partial t} - \mathcal{L}_k F_k \right) dxdy = 0, \qquad \text{for } k = 1, \cdots, r \tag{4}$$

In general, (4) leads to a system of nonlinear equations for the unknowns $\{\alpha_{k,ij}\}$ $(k = 1, \cdots, r;\ i,j = 0, 1, \cdots, N+1)$. However, as we shall see, only a linear algebraic system needs to be solved if we use a semi-implicit time stepping scheme.

3 A semi-implicit time stepping scheme

Let us consider a model equation of the one dopant case

$$\frac{\partial f}{\partial t} = D \cdot \text{Div}(\text{grad} f) + (V_1, V_2) \cdot \text{grad} f \tag{5}$$

Then the generalization of the predictor corrector scheme of [1, §4] to the 2D case takes the following form

$$\begin{cases} \frac{f^{j+\theta}-f^j}{\theta\Delta t} = D\cdot \mathrm{Div}(\mathrm{grad} f^{j+\theta}) + (V_1, V_2)\cdot \mathrm{grad} f^j \\ \frac{f^{j+2}-f^j}{2\Delta t} = D\cdot \mathrm{Div}(\mathrm{grad} f^{j+2}) + (V_1, V_2)\cdot \mathrm{grad} f^{j+\theta} \end{cases} \tag{6}$$

To carry out a stability analysis of (6), we further approximate it by the finite difference method leading to

$$\begin{cases} \frac{f^{j+\theta}_{mn}-f^j_{mn}}{\theta\Delta t} = D\left(\frac{\delta_x^2}{\Delta x^2}+\frac{\delta_y^2}{\Delta y^2}\right) f^{j+\theta}_{mn} + \left(V_1\frac{\delta_x}{2\Delta x}+V_2\frac{\delta_y}{2\Delta y}\right) f^j_{mn} \\ \frac{f^{j+2}_{mn}-f^j_{mn}}{2\Delta t} = D\left(\frac{\delta_x^2}{\Delta x^2}+\frac{\delta_y^2}{\Delta y^2}\right) f^{j+2}_{mn} + \left(V_1\frac{\delta_x}{2\Delta x}+V_2\frac{\delta_y}{2\Delta y}\right) f^{j+\theta}_{mn} \end{cases} \tag{7}$$

where the usual finite difference operators are defined by

$$\begin{cases} \delta_x^2 f^\tau_{mn} = f^\tau_{m+1,n} + f^\tau_{m-1,n} - 2f^\tau_{m,n} \\ \delta_y^2 f^\tau_{mn} = f^\tau_{m,n+1} + f^\tau_{m,n-1} - 2f^\tau_{m,n} \\ \delta_x f^\tau_{mn} = f^\tau_{m+1,n} - f^\tau_{m-1,n} \\ \delta_y f^\tau_{mn} = f^\tau_{m,n+1} - f^\tau_{m,n-1} \end{cases}$$

Further we have

THEOREM 1 *(2D stability)*

The predictor corrector scheme (6) is stable for any $\theta > 0$, provided that

$$\Delta t \le \min\left(\frac{D}{V_1^2}, \frac{D}{V_2^2}\right).$$

Proof. Use the usual von Neumann (Fourier) analysis along similar lines of the proof of Theorem 1 of [1]. □

4 Local truncation error analysis

We shall now apply the finite element method of §2 to the model equation (5) combined with the time stepping scheme (6) and further analyze the local truncation error. Estimates of truncation errors can be used in designing a practical time step selection strategy (see §5).

Figure 1: 9 point stencil for variable α.

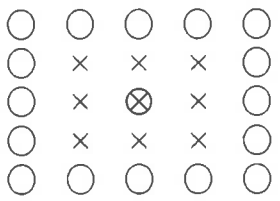

Integrating the corrector equation of (6) over box Ω_{lm}, we obtain the following ASWR equation

$$\frac{1}{2\Delta t}\int_{\Omega_{lm}}(f^{j+2}-f^{j})dxdy = D\int_{\Omega_{lm}}\mathrm{Div}(\mathrm{grad}f^{j+2})dxdy + \int_{\Omega_{lm}}(V_1,V_2)\mathrm{grad}f^{j+\theta}dxdy \quad (8)$$

where $f^{\tau}=\sum\alpha_{i,k}^{\tau}D_{ik}(x,y)$. Taking into consideration the piecewise behaviour of D_{ik}, we get

$$\begin{aligned}&\sum_{i=l-1}^{l+1}\sum_{k=m-1}^{m+1}\frac{\alpha_{i,k}^{j+2}-\alpha_{i,k}^{j}}{2\Delta t}\int_{\Omega_{lm}}D_{ik}(x,y)dxdy\\ &= D\sum_{i=l-1}^{l+1}\sum_{k=m-1}^{m+1}\alpha_{i,k}^{j+2}\int_{\Omega_{lm}}\mathrm{Div}(\mathrm{grad}D_{ik})dxdy + \sum_{i=l-1}^{l+1}\sum_{k=m-1}^{m+1}\alpha_{i,k}^{j+\theta}\int_{\Omega_{lm}}(V_1,V_2)\mathrm{grad}D_{ik}dxdy\end{aligned} \quad (9)$$

Now direct calculations of the above coefficients simplify (9) to

$$\begin{aligned}&\frac{\delta_t}{72\Delta t}\Big[\alpha_{l-1,m-1}^{j+2}+\alpha_{l+1,m-1}^{j+2}+\alpha_{l-1,m+1}^{j+2}+\alpha_{l+1,m+1}^{j+2}\\ &\quad+4(\alpha_{l,m-1}^{j+2}+\alpha_{l,m+1}^{j+2}+\alpha_{l-1,m}^{j+2}+\alpha_{l+1,m}^{j+2})+16\alpha_{l,m}^{j+2}\Big]\\ &=\frac{D}{3\Delta x^2}\Big[\alpha_{l-1,m-1}^{j+2}+\alpha_{l+1,m-1}^{j+2}+\alpha_{l-1,m+1}^{j+2}+\alpha_{l+1,m+1}^{j+2}\\ &\qquad+\alpha_{l,m-1}^{j+2}+\alpha_{l,m+1}^{j+2}+\alpha_{l-1,m}^{j+2}+\alpha_{l+1,m}^{j+2}-8\alpha_{l,m}^{j+2}\Big]\\ &\quad+\frac{V_1}{2\Delta x}\Big[(\alpha_{l+1,m+1}^{j+\theta}-\alpha_{l-1,m+1}^{j+\theta})+(\alpha_{l+1,m-1}^{j+\theta}-\alpha_{l-1,m-1}^{j+\theta})+4(\alpha_{l+1,m}^{j+\theta}-\alpha_{l-1,m}^{j+\theta})\Big]\\ &\quad+\frac{V_2}{2\Delta y}\Big[(\alpha_{l+1,m+1}^{j+\theta}-\alpha_{l+1,m-1}^{j+\theta})+(\alpha_{l-1,m+1}^{j+\theta}-\alpha_{l-1,m-1}^{j+\theta})+4(\alpha_{l,m+1}^{j+\theta}-\alpha_{l,m-1}^{j+\theta})\Big]\end{aligned} \quad (10)$$

where $\delta_t\beta^{j+2}=\beta^{j+2}-\beta^{j}$. The computational stencil of nine points is shown in Fig.1. To find the local truncation error for (10), we may use the Taylor theorem. Unfortunately the

unknowns (α's) are not the solution functions (f). They are only related to the solution by the following interpolation relationship

$$\sum_{i=l-1}^{l+1} \sum_{k=m-1}^{m+1} \alpha_{i,k}^{\tau} D_{ik}(\bar{x}_l, \bar{y}_m) = f(t_\tau, \bar{x}_l, \bar{y}_m) \tag{11}$$

where $(\bar{x}_l, \bar{y}_m)$ is taken to be the centre point of box Ω_{lm} for $l, m = 1, \cdots, N$. For the Dirichlet boundary condition $f(t, x, y)|_{\partial\Omega} = 0$, the above system may be written as

$$F\alpha^{\tau} \equiv \frac{1}{72} \begin{pmatrix} U_0 & U_1 & & & \\ U_1 & U_2 & U_1 & & \\ & \ddots & \ddots & \ddots & \\ & & U_1 & U_2 & U_1 \\ & & & U_1 & U_0 \end{pmatrix} \begin{pmatrix} \alpha_{1,1}^{\tau} \\ \alpha_{1,2}^{\tau} \\ \vdots \\ \alpha_{N,N}^{\tau} \end{pmatrix} = \begin{pmatrix} f_{1,1}^{\tau} \\ f_{1,2}^{\tau} \\ \vdots \\ f_{N,N}^{\tau} \end{pmatrix} \tag{12}$$

where

$$U_1 = \begin{pmatrix} 6 & 1 & & & \\ 1 & 7 & 1 & & \\ & \ddots & \ddots & \ddots & \\ & & 1 & 7 & 1 \\ & & & 1 & 6 \end{pmatrix}, \qquad U_2 = \begin{pmatrix} 23 & 7 & & & \\ 7 & 40 & 7 & & \\ & \ddots & \ddots & \ddots & \\ & & 7 & 40 & 7 \\ & & & 7 & 23 \end{pmatrix},$$

$$U_0 = \begin{pmatrix} 27 & 6 & & & \\ 6 & 33 & 6 & & \\ & \ddots & \ddots & \ddots & \\ & & 6 & 33 & 6 \\ & & & 6 & 27 \end{pmatrix}$$

The matrix F can be seen to be diagonally dominant and in block tridiagonal form. The elements of the inverse of such a matrix are known to decay exponentially to zero in magnitude away from the main diagonal. Refer to Demko et al [2] and Meurant [8].

By calculating the inverse F^{-1} numerically, we can express the unknowns $\alpha_{i,k}^{\tau}$'s in terms of the solution (RHS vector) $f_{i,k}^{\tau}$'s. Here we propose to use a band approximation of F^{-1} to solve equation (12) by neglecting those subdiagonal entries of F^{-1} away from the main diagonal which are less than some small positive number ε in magnitude. This

Figure 2: 25 point stencil for variable f (with each α).

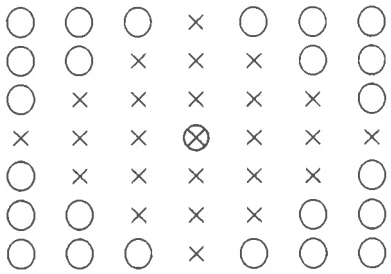

enables us to express accurately the $\alpha^{\tau}_{i,k}$'s in terms of local $f^{\tau}_{i,k}$'s. For (12), such an approximation is given by (taking $\varepsilon = 10^{-2}$)

$$\begin{aligned}\alpha^{\tau}_{l,m} = 10^{-4}\big[&-133(f^{\tau}_{l,m-3} + f^{\tau}_{l,m+3} + f^{\tau}_{l-3,m} + f^{\tau}_{l+3,m})\\ &-185(f^{\tau}_{l-1,m-2} + f^{\tau}_{l-1,m+2} + f^{\tau}_{l+1,m-2} + f^{\tau}_{l+1,m+2}\\ &\quad + f^{\tau}_{l-2,m-1} + f^{\tau}_{l-2,m+1} + f^{\tau}_{l+2,m-1} + f^{\tau}_{l+2,m+1})\\ &+831(f^{\tau}_{l,m-2} + f^{\tau}_{l,m+2} + f^{\tau}_{l-2,m} + f^{\tau}_{l+2,m})\\ &+852(f^{\tau}_{l-1,m-1} + f^{\tau}_{l-1,m+1} + f^{\tau}_{l+1,m-1} + f^{\tau}_{l+1,m+1})\\ &-3830(f^{\tau}_{l,m-1} + f^{\tau}_{l,m+1} + f^{\tau}_{l-1,m} + f^{\tau}_{l+1,m})\\ &+20600 f^{\tau}_{l,m}\end{aligned} \tag{13}$$

The computational stencil of 25 f points for each $\alpha^{\tau}_{l,m}$ is shown in Fig.2. The availability of $\alpha^{\tau}_{i,k}$'s (for $\tau = j, j+\theta, j+2$) from (13) allows us to work out the local truncation error of (10) in a straightforward manner. This has been found to be

$$\tau(t_j, \bar{x}_l, \bar{y}_m) = R_0\Delta t + R_{11}\Delta x^2 + R_{12}\Delta x\Delta y + R_{22}\Delta y^2 + \cdots \tag{14}$$

where

$$\begin{aligned}R_0 &= E_1 - \theta E_2;\\ E_1 &= \left(V_1\frac{\partial}{\partial x} + V_2\frac{\partial}{\partial y}\right)^2 f - D^2\nabla^2(\nabla^2 f);\\ E_2 &= \left(V_1\frac{\partial}{\partial x} + V_2\frac{\partial}{\partial y}\right)^2 f - D^2\left(V_1\frac{\partial}{\partial x} + V_2\frac{\partial}{\partial y}\right)\nabla^2 f;\\ R_{11} &= \frac{D}{6}\frac{\partial^2}{\partial x^2}\nabla^2 f - \frac{D}{12}\frac{\partial^4 f}{\partial x^4};\\ R_{12} &= -\frac{D}{3}\frac{\partial^4 f}{\partial x^2\partial y^2};\\ R_{22} &= \frac{D}{6}\frac{\partial^2}{\partial y^2}\nabla^2 f - \frac{D}{12}\frac{\partial^4 f}{\partial y^4}.\end{aligned}$$

In a typical semiconductor diffusion model, the potential term Φ is also present and the equation corresponding to (5) is of the following form

$$\frac{\partial f}{\partial t} = D \cdot \mathrm{Div}(\mathrm{grad}(f + Z\Phi)) + [(\bar{V}_1, \bar{V}_2) + ZD\mathrm{grad}\Phi]\mathrm{grad}f \tag{15}$$

The above equation may be identified with (5) with the perturbation of $f = f + ZD \cdot \mathrm{Div}(\mathrm{grad}\Phi)$ and $V_1 = \bar{V}_1 + ZD\frac{\partial \Phi}{\partial x}$ and $V_2 = \bar{V}_2 + ZD\frac{\partial \Phi}{\partial y}$. Therefore time step selection strategies of the next section can be used for solving equation (15). In order to apply our model analysis to the full nonlinear equation

$$\frac{\partial f}{\partial t} = \mathrm{Div}\,[D\mathrm{grad}(f + Z\Phi)] + D\mathrm{grad}f \cdot \mathrm{grad}(f + Z\Phi) \tag{16}$$

local linearizations have to be introduced. For example, the diffusion coefficient D may be viewed as locally constant and $(V_1, V_2) = D\mathrm{grad}(f + Z\Phi)$ may be defined so that the linear analysis is applicable.

We next consider the selection of time step Δt based on these truncation error estimates.

5 Time step selection

The automatic selection of the time step Δt follows the principle that the temporal error (Δt term) should be of comparable magnitude to the spatial discretization error (Δx and Δy terms). In this way, the overall error is determined only by the spatial discretization accuracy.

Apart from using the errors in certain equation variables, we shall also consider the

relative mass balance error. This quantity is defined at time t by

$$Q_t = \frac{(M_t - M_0)}{M_0} \tag{17}$$

where M_0 and M_t denote the total mass present in the silicon at time 0 and t respectively. Here the total mass at time $t = t_j$ is defined based on the numerical solution f^j by

$$M_t = \int_\Omega C^j(x,y)dxdy \equiv \int_\Omega \exp[f^j(x,y)]dxdy \tag{18}$$

We wish to have *mass conservation* of the total mass M_t, which is of physical importance. By this we mean that $M_t = M_0$ at any time t. If the underlying PDE is of the conservation form such as (1) in C, then most numerical methods (including the Euler scheme) for solving such an equation will conserve the total mass. But our transformed PDE (2) in f is not of conservation form. Conservation of mass in f as well as $\exp(f)$ cannot be maintained in general. We hope to conserve the mass as much as possible numerically by suitably choosing the time step Δt once given *a priori* spatial discretizations.

5.1 Error control in f

This approach is, as introduced in [1, §4.4], to use the transformed equation (5) in variable f. For equation (5), the time step selection based on (14) should satisfy

$$\Delta t \leq \mathrm{TOL}/\max|R_0| \tag{19}$$

where TOL is chosen to be proportional to the estimate of $|R_{11}\Delta x^2 + R_{12}\Delta x\Delta y + R_{22}\Delta y^2|$. Of course, the above choice should also be subject to the stability condition of Theorem 1 being satisfied.

5.2 Mass Error control in C

The idea is first to relate the local truncation error of §4 to the dopant mass error, and then to identify contributions from temporal and spatial discretizations in such a mass error in order to select an appropriate time step.

Assume that stability is satisfied throughout our calculations. Then the following relation holds for the global error

$$f - f^{j+2} = K\tau + O(\Delta t^2) \tag{20}$$

where $f = f(x, y, t_{j+2})$ and f^{j+2} represent respectively the exact and numerical solution at time level $j+2$, K is a stability constant, τ is the local truncation error (see (14)) and $O(\Delta t^2)$ denotes the negligible high order error terms. Note from §1 that $C = \exp(f)$ and $C^{j+2} = \exp(f^{j+2})$. Taking the exponential of both sides of (20) gives rise to

$$C = C^{j+2} \exp[K\tau + O(\Delta t^2)] \tag{21}$$

Now integrate both sides of (21) over the entire domain to get

$$M_0 = M_t + \int_\Omega \exp[f^{j+2}] \left\{ \exp[K\tau + O(\Delta t^2)] - 1 \right\} dxdy \tag{22}$$

where we have used the definitions of (17) and (18).

We shall try to conserve the total mass, *i.e.* to minimise $M_0 - M_t$ while allowing the largest possible time step Δt for efficiency. Define the mass error by

$$\mathrm{ME} = M_0 - M_t \equiv \int_\Omega \exp[f^{j+2}] \left\{ \exp[K\tau + O(\Delta t^2)] - 1 \right\} dxdy \tag{23}$$

whose leading term on expansion is

$$\mathrm{ME}_1 = K \int_\Omega \exp[f^j] \left(R_0 \Delta t + \mathrm{SE} \right) dxdy \tag{24}$$

where substitution of (14) has been performed and the spatial error is denoted by SE = $R_{11}\Delta x^2 + R_{12}\Delta x\Delta y + R_{22}\Delta y^2$. More specifically, equation (24) can be rewritten as

$$\mathrm{ME}_1 = K(\mathrm{ME}_t + \mathrm{ME}_s) \tag{25}$$

with $\mathrm{ME}_t = \Delta t \int_\Omega \exp[f^j] R_0 dxdy$ and $\mathrm{ME}_s = \int_\Omega \exp[f^j]\mathrm{SE}dxdy$ representing mass error contributions from temporal and spatial discrtizations respectively.

The strategy based on mass error control is to equidistribute the total mass error ME in time and space by forcing

$$\mathrm{ME}_t = \mathrm{ME}_s$$

i.e. by selecting the time step

$$\Delta t = \int_\Omega \exp[f^j]\mathrm{SE}dxdy \Big/ \int_\Omega \exp[f^j] R_0 dxdy \tag{26}$$

5.3 Choice of the predictor step

The choice of the predictor step may be arbitrary as far as the stability of the predictor corrector scheme (6) is concerned (see Theorem 1). The idea here is to minimise in some sense a measure of the solution error. We have considered two approaches.

The first one follows from that of [1, §4.4.1] based on minimization of the local truncation error. As θ is a constant appearing in the pointwise local truncation error estimates, we cast the problem of choosing θ as a minimisation problem in the least squares sense. See [1, §4.4.1].

The second approach is to track the mass balance history and dynamically adjust θ from step to step in order to achieve mass conservation; see [7]. To illustrate, let us define

at time $t = t_j$ the *approximate* total mass in the silicon medium Ω by

$$m_j = \sum_{l=1}^{N} \sum_{m=1}^{N} \exp[\bar{x}_l, \bar{y}_m, f(t_j)] \Delta x_l \Delta y_m \tag{27}$$

and the relative j-th step mass error by

$$B_j = (m_j - m_{j-1})/m_{j-1} \tag{28}$$

where m_j is the result of (18) applied with the mid-point quadrature rule. Using $\theta_0 = 1$, it has been proposed in [7] to use

$$\theta_j = \theta_{j-1}(1 + 100 B_j) \tag{29}$$

if $B_j > 0$ and $B_j > B_{j-1}$ and

$$\theta_j = \theta_{j-1}[1 - 100(B_{j-1} - B_j)] \tag{30}$$

if $B_j > 0$ and $B_{j-1} - B_j < B_j/3$. Similar choices are made for the case of $B_j < 0$, otherwise set $\theta_j = \theta_{j-1}$.

In the next section, we shall experiment on our time step selection strategy using both the minimization and mass balance choices for the predictor step.

6 Numerical experiments

We have taken four typical semiconductor processing structures as shown in Figs.3-6. The initial profiles for our test problems are obtained from the Ion Implantation Menu of COMPOSITE [6], which are Pearson IV distributions. Detailed data specifications are shown in Table 1, where Test 5 and 6 use two dopants.

Figure 3: Substrate for Test examples 1 and 2

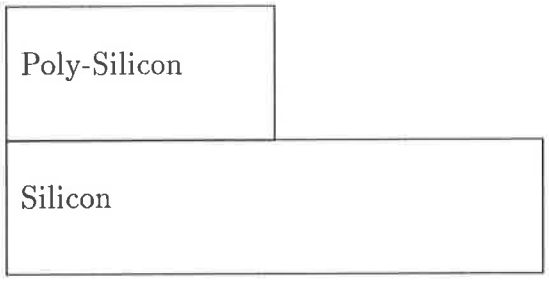

Figure 4: Substrate for Test example 3

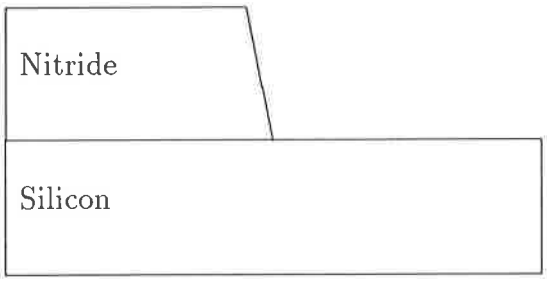

We have run all six test examples with both the existing ASWR method of [7] and our modified version of the ASWR method. With our modified version, we have used the following strategies :

- For Boron/Phosphorus/Antimony implants, the selection method of §5.1 is used;
- For Arsenic implant, the selection method of §5.2 is used;
- The predictor step uses the second approach of §5.3.

We remark that the above combination of ideas offers a robust method from experimental observations, although it gives by no means the best results in some cases. The numerical results are summarised in Table 2, where information on the number of time steps taken, the CPU user time of SUN-4 and the mass balance error Q_t is given. The mesh data given are for the finite difference (FD) mesh, and the number of boxes for the finite element (FE) discretization is about half of the number of FDM mesh lines in both directions.

For example, an 65×65 FD mesh corresponds to [(65-1)/]2 × [(65-1)/2] FE boxes. The diffused profiles by the modified ASWR method are shown in Figs.7-12.

Results have clearly demonstrated that our modified time stepping strategy generally shows better performance compared with the existing ASWR strategy, which uses heuristic time stepping ideas (see [7]). Our method of estimating the local truncation errors of the ASWR finite element method appears to be new and simple.

Acknowledgement

Financial support from the Department of Trade and Industry (DTI) through the Science and Engineering Research Council (SERC) is gratefully acknowledged.

References

[1] K. CHEN, M. J. BAINES & P. K. SWEBY, "On time step selection for solving 1D nonlinear diffusion equations", Numerical Analysis Report, **10/91**, Dept of Mathematics, University of Reading, 1991.

[2] S. DEMKO, W. F. MOSS & P. W. SMITH, "Decay rates for inverses of band matrices", *Math. Comp.*, **43**(188), 491-499, 1984.

[3] K. ERIKSSON & C. JOHNSON, "Error estimates and automatic time step control for nonlinear parabolic problems, I", *SIAM J. Numer. Anal.*, **24**(1), 12-23, 1987.

[4] J. P. KRESKOVSKY & H. L. GRUBIN, "Application of LBI techniques to the solution of the transient, multidimensional semiconductor equations", *J. Comput. Phys.*, *68*, 420-461, 1987.

[5] J. D. LAMBERT, *Computational methods in ordinary differential equations*, Wiley, 1973.

[6] J. LORENZ, J. PELKA, H. RYSSEL, A. SACH, A. SEIDEL & M. SVOBODA, "COMPOSITE – a complete modeling program of silicon technology", *IEEE Trans. Elec. Dev.*, **ED-32**(10), 1977-1986, 1985.

Figure 5: Substrate for Test example 4

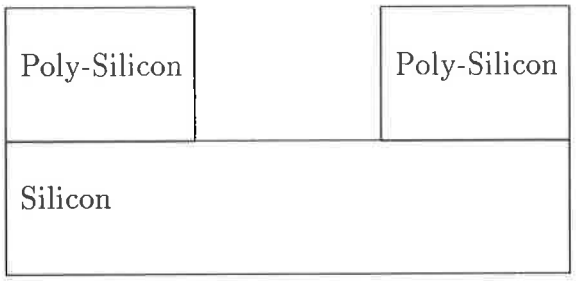

Figure 6: Substrate for Test example 5 and 6

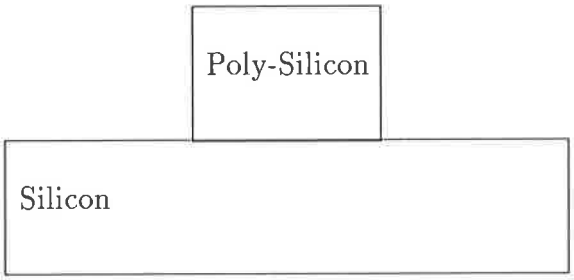

[7] J. LORENZ & M. SVOBODA, "ASWR - method for the simulation of dopant redistribution in silicon", in *Simulation of Semiconductor Devices and Processes*, **3**, eds. G. Daccarani et al., 243-254, Tecnoprint, 1988.

[8] G. MEURANT, "A review on the inverse of symmetric tridiagonal and block tridiagonal matrices", to appear in *SIAM J. Appl. Math.*, 1991.

[9] R. R. O'BRIEN, C. M. HSIEH, J. S. MOORE, R. F. LEVER, R. F. MURLEY, K. W. BRANNON, G. R. SRINIVASAN & R. W. KNEPPER, "Two-dimensional process modelling : a description of the SAFEPRO program", *IBM J. Res. Dev.*, **29**(3), 1985.

[10] M. SVOBODA, "A Petrov-Galerkin procedure for simulation of solid-state diffusion in semiconductor fabrications", Ph.D. thesis, Faculty of Mathematics, Ludwig Maximillians University, Munich, Germany, 1988.

Table 1: Ion Implantation and Diffusion Data

Test	Dopants	Energy (Kev)	Dose(cm^{-2})	Temperature /	Time (Min)
1	Boron	30	1.0E12	1000	40
2	Phosphorus	50	1.0E15	1000	50
3	Antimony	25	1.0E14	1100	2
4	Arsenic	40	1.0E14	1100	2
5	Boron	30	1.0E13	1100	1
	Phosphorus	25	1.0E12		
6	Boron	20	1.0E12	1000	5
	Phosphorus	50	1.0E15		

Table 2: ASWR test results of six examples

Method	Test	Mesh	Time Steps	CPU	Error Q_t
Existing ASWR	1	85×85	30	535	1.5E-3
	2	65×65	123	1290	-7.6E-4
	3	65×65	86	971	-1.3E-3
	4	129×129	69	3000	-3.3E-4
	5	85×85	62	2000	-1.0E-3
					-5.0E-2
	6	65×65	50	992	-1.1E-2
					1.9E-3
Modified ASWR	1	85×85	13	277	2.8E-3
	2	65×65	43	574	2.4E-5
	3	65×65	28	428	-1.9E-4
	4	129×129	59	2890	-1.5E-4
	5	85×85	22	1150	2.0E-3
					1.5E-3
	6	65×65	16	443	-4.7E-3
					-5.7E-4

Figure 7.

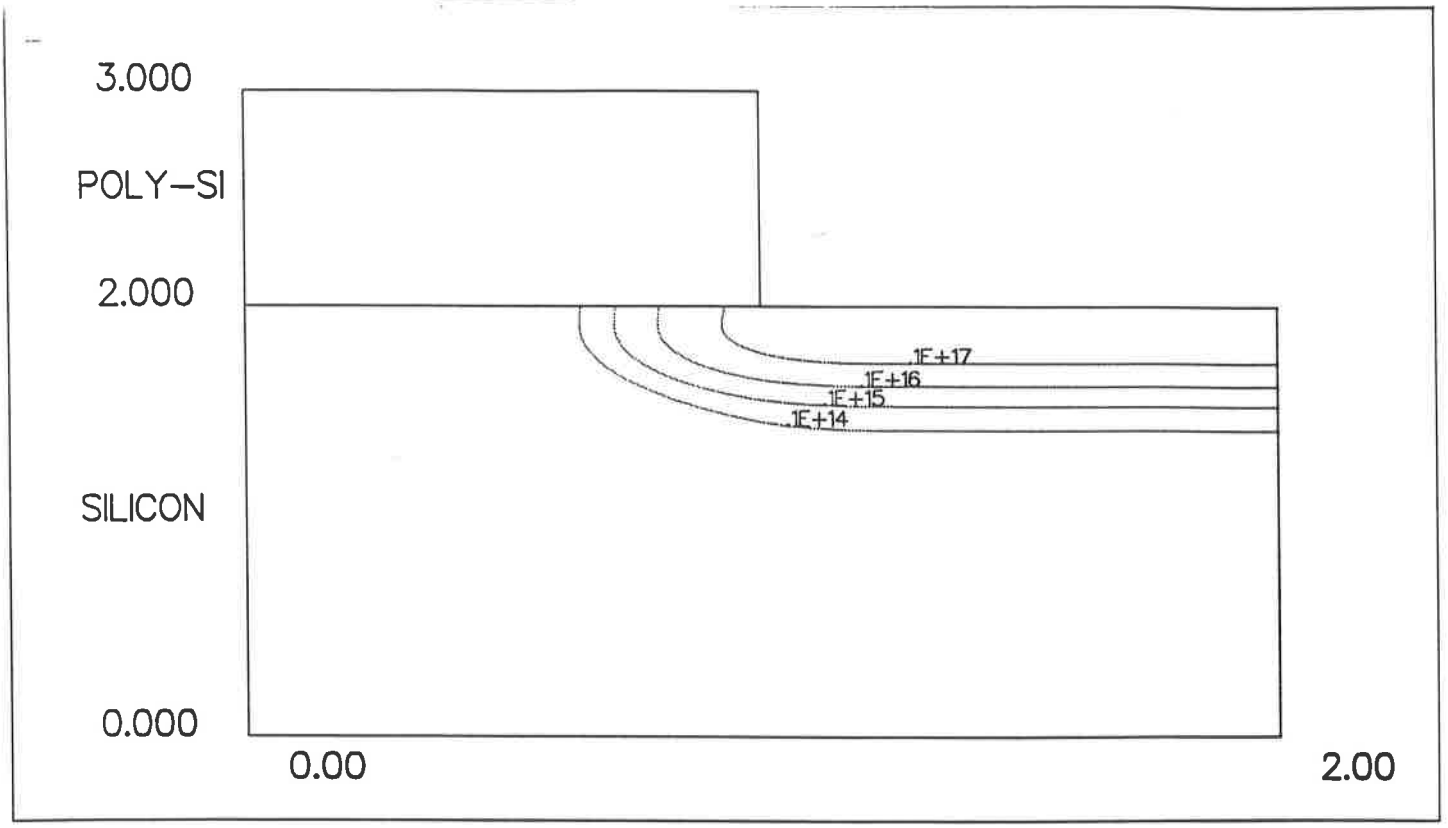

Figure 8.

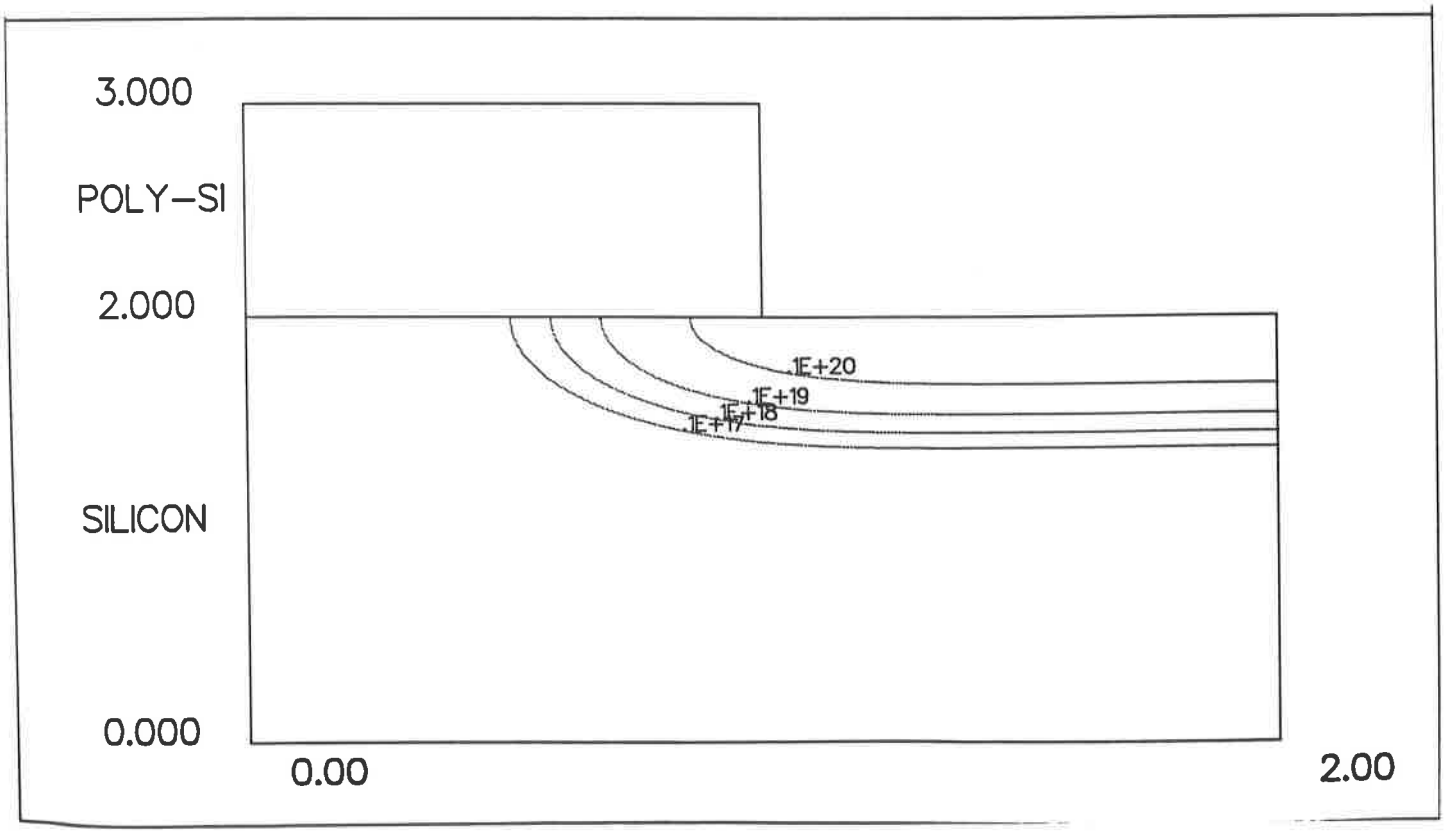

Figure 9.

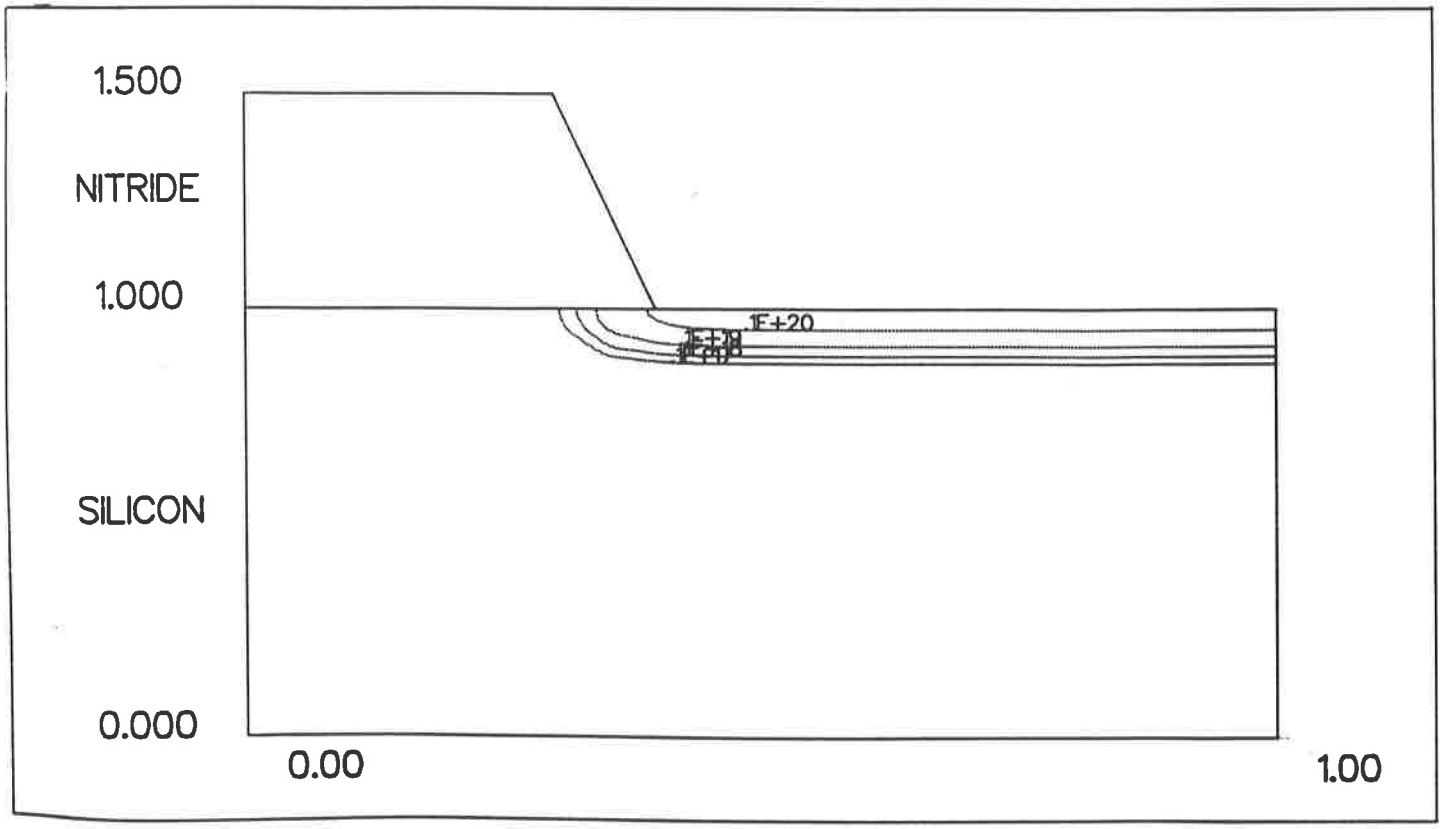

Figure 10.

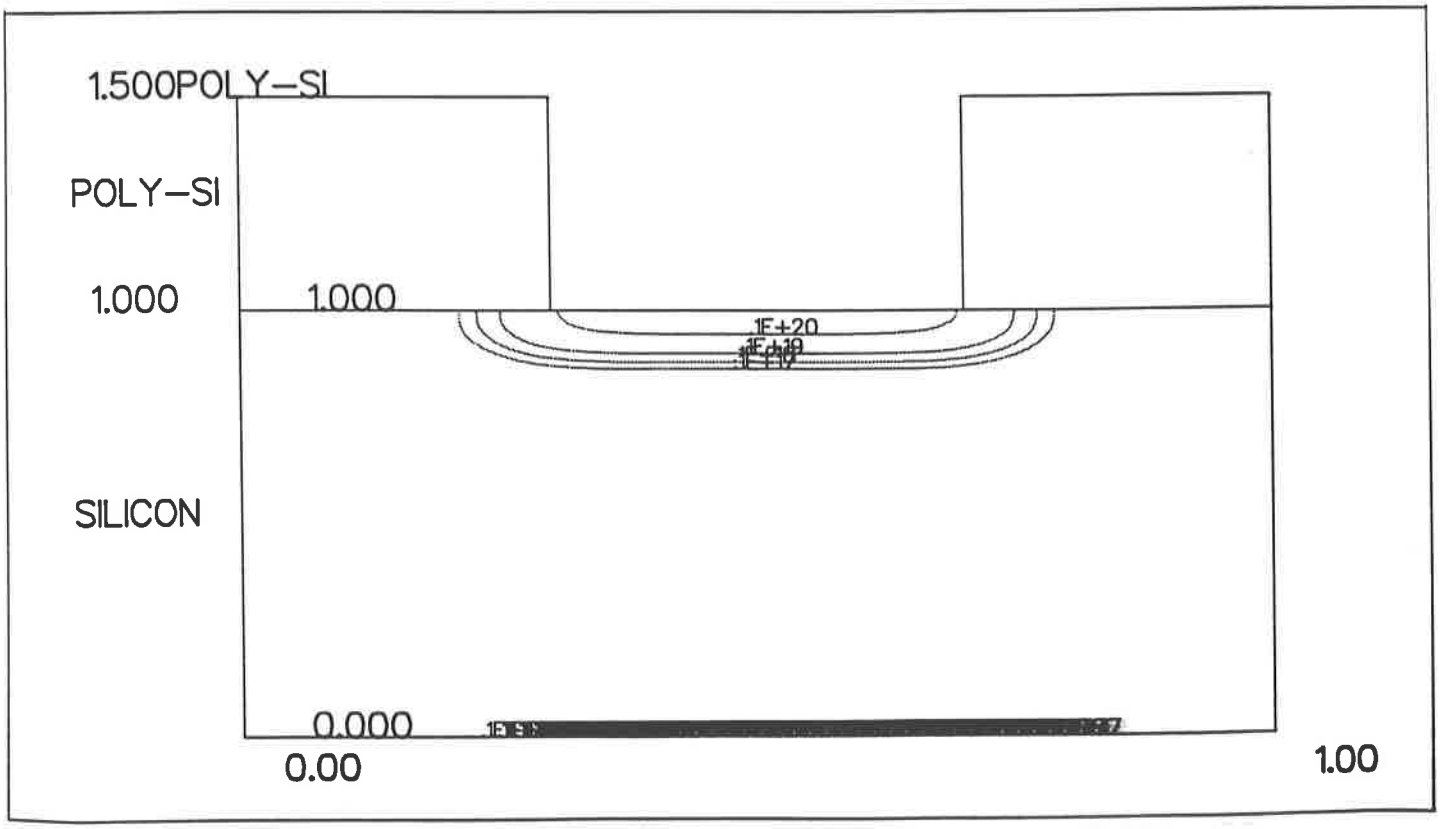

Figure 11.

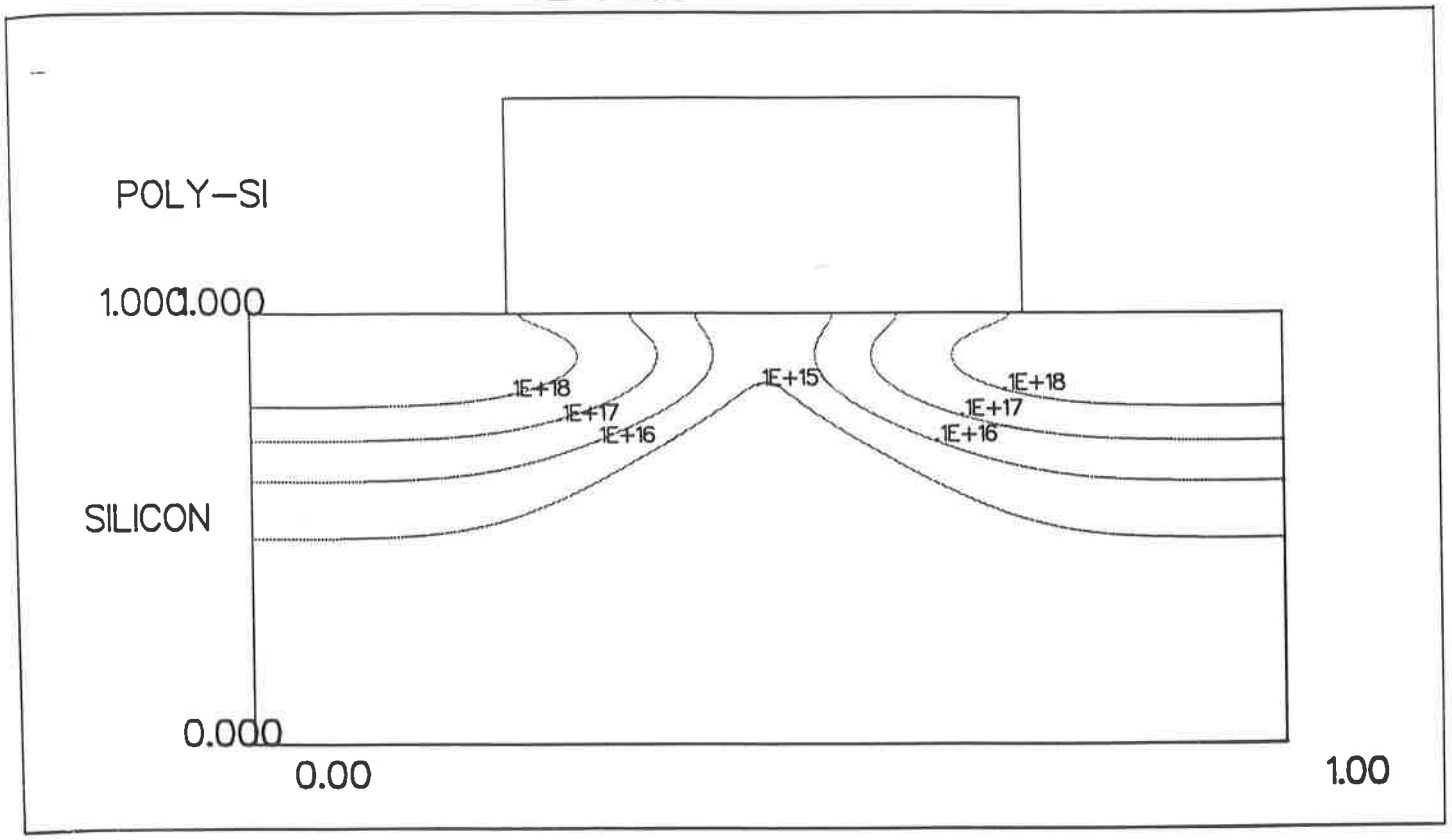

Figure 12.